

EFFECT OF INCLUSIONS ON THE TENSILE PROPERTIES INSIDE A LPPM A356 CASTING

Franco Chiesa, David Levasseur, and Guy Morin

Centre de métallurgie du Québec, Trois-Rivières, QC, Canada

Bernard Duchesne

Collège de Trois-Rivières, Trois-Rivières, QC, Canada

Copyright © 2016 American Foundry Society
DOI 10.1007/s40962-016-0029-3

Abstract

Contrary to metallurgical properties such as dendrite fineness or microporosity, the level of inclusions in a casting is difficult if not impossible to assess accurately. Consequently, it is not easy to quantify the detrimental effect of inclusions on tensile properties. In the present work, this has been attempted on an aluminum A356 step casting, the geometry of which offers a wide range of solidifying conditions. It was poured in low pressure permanent mold, a process which minimizes the variability of mold filling. The interaction between the melt gas content and inclusions in producing microporosity was highlighted by analyzing reduced pressure test samples. Radiographic analyses and die penetrant checks were performed to detect microshrinkage and inclusions in the castings. The

effect of inclusions on tensile properties was assessed by separating tensile samples in which inclusions were observed in the fracture surface from those with a flawless fracture surface. It was thus possible to compare tensile properties with and without inclusions in the same casting. This procedure eliminated the variability introduced by the numerous additional factors bearing on the tensile properties such as the chemical composition, melt preparation and heat treatment. This distinguishes the present study from those previously carried out on the influence of inclusions on tensile properties.

Keywords: aluminum, inclusions, tensile properties

Introduction

Aluminum silicon magnesium alloys are the workhorse of casting alloys for their excellent castability, their response to heat treatment and their resistance to atmospheric corrosion. Alloy A356 (7 % Si, 0.4 % Mg) has been extensively used for the past 50 years without drastic changes in its composition. However, a continuous improvement in its metallurgical quality has been achieved over the years via the reduction of deleterious elements such as Fe in electrolytic cells and post treatments in cast houses; the abatement of inclusions all along the cast-house production process and melt treatment, such as degassing, grain refining and modification in the foundry. The quality of aluminum A356 casting is normally assessed by:

1. Spectrographic analysis, the results of which must meet specifications, particularly for elements Si, Mg, Mn, Cr and Ti. Fe and Cu contents should be as low as possible for better ductility and corrosion resistance.
2. Level of microporosity which will affect the mechanical properties and radiographic quality. Microporosity can only be measured on an excision of the casting; a level below 0.7 % will normally secure a “frame 1” rating per American Society for Testing and Materials (ASTM E155 while levels beyond 1.5 % are usually unacceptable (corresponding to “frame 4” per ASTM 155).
3. Dendrite fineness, as measured by the dendrite arm spacing (DAS); it only depends on the local solidification time, hence on the casting geometry and process (sand vs. permanent mold, use of chills or local thermal devices).

A version of this paper was published in 2015 AFS Transactions.

All the above properties are easy to quantify and can be readily compared to the “best practice” properties. The case of inclusions content is much more problematic as their nature, size and content are not readily measurable, in the melt and in the solidified casting as well.

Methods do exist to quantify inclusion levels, at least comparatively; however, they are not practical for use in a foundry. They include:

- LiMCA¹ (Liquid Metal Cleanliness Analyzer), which is a costly apparatus used in aluminum smelter cast-houses, normally in a continuous process;
- PoDFA² (Porous Disc Filtration Analysis,) which is a lengthy laboratory procedure and
- Prefil-Footer, designed for online usage³ but shown problematic in a batch process.⁴

In shape casting foundries, the most widespread tool to indirectly assess the cleanliness of the melt is the reduced pressure test (RPT) where the density of a sample solidifies under partial vacuum. This test is generally thought to measure the amount of hydrogen dissolved in the melt, which is true only to an extent. The RPT test doesn't quantify the amount of H dissolved in the melt like an AlScan probe would,⁵ but measures the combination of gas and inclusion contents as has clearly been shown previously.⁶ Hydrogen gas is very difficult to nucleate homogeneously from a clean hydrogen supersaturated melt; an oxide substrate is necessary for H₂ bubbles to form. It is even argued that a gassed melt would produce no porosity in the absence of inclusions.⁷

If inclusions are difficult to quantify in the melt, the problem becomes even more challenging in the solidified casting. In this case, the two methods available to detect inclusion are:

- Neutron activation, often adulterated by the oxide layer that always exists at the surface of the sample.
- Die penetrant checks, which only detect inclusions open to the surface of the sample if the test is to remain non-destructive. In the present work, this technique is used to highlight the presence and shape of internal inclusions by slicing into the castings.

Among inclusions, only the three dimensional ones, a few hundred micrometers in size, will be visible on radiographs (foreign material less dense per ASTM E155). Two dimensional inclusions preexisting in the melt and bifilms produced during filling do not appear on a radiographic image.

In contrast, inclusions responsible for the failure of a tensile test bar are easy to spot on the fracture surface, its dull appearance contrasting sharply with the shiny metallic

surface. This makes it possible to quantify the loss in mechanical property when, in a casting, the breakage is induced by an inclusion visible on the fracture surface.

Numerous works have been carried out on the effect of inclusions on mechanical properties of aluminum casting alloys. A comprehensive review of the situation is currently available.⁸ Among most recent works, one compared the reproducibility of tensile properties of sand cast 20 mm (0.79 in.) diameter bars produced from filtered and unfiltered gating systems.⁹ In another study, the melt was dirtied by adding turnings in order to assess the influence of inclusions, the level of which was quantified by running PoDFA tests.¹⁰ However, in most previous studies, comparisons were carried out on different castings sometimes produced from different melts.¹¹ The novelty of the present work was to compare inside the same casting, the tensile properties of samples where an inclusion is detected in the fracture surface to those of samples where no inclusion was observed. Here lies the originality in our method—it will reduce the effect of the many additional factors influencing tensile properties, however identical these factors are supposed to be from one test to the next (composition, melt treatment, time of pour, gas content, etc.). Pouring the castings via the Low Pressure Permanent Mold (LPPM) process also improves repeatability of the filling process as compared to gravity casting.

Pouring the Castings

Stepped castings, 150 mm (5.94 in.) wide and 6 mm (0.24 in.), 12 mm (0.47 in.) and 25 mm (0.98 in.) in thickness were poured by the low pressure permanent mold process at 740 °C (1364 °F) in the cast iron mold, shown in Figure 1. They were produced from the same melt made up of



Figure 1. The mold is mounted on LPPM press.

100 % small returns (gates) so as to contain a fair amount of inclusions. Thirteen such castings were cast (Figure 2) and castings #6–#11 were set aside for the present study (It had been previously determined that 5 pours were necessary to bring the process to a dynamic thermal steady state).

By calibrating solidification modeling to thermocouple readings inside the cavity, it was determined that the local solidification time at the center of the 6 mm (0.24 in.), 12 mm (0.47 in.) and 25 mm (0.98 in.) plates were 10, 31 and 54 s, respectively.

Melt Treatment

The chemistry of the recycled melt was as follows:

6.70Si 0.10Fe 0.03Cu 0.01Mn 0.33Mg 0.01Zn 0.12Ti
0.011Sr

The melt was degassed (no fluxing) to a level of 0.08 ml H₂/100 g as measured by an Alscan probe. In spite of this thorough degassing, the (RPT) sample density was low (2.49) due to the nucleating effect of the inclusions. Figure 3 compares the RPT sample section of the ‘dirty’ melt, to that of a clean argon degassed melt with a similar gas content (0.05 ml H₂/100 g). The clean melt sample is on the left, the bottom picture showing a radiographic shot of the two samples. The radiograph indicated that the huge difference in density between the two samples does not show much on the cross sections.

These results are in keeping with the fact that, in the absence of inclusions, molecular hydrogen bubbles will not nucleate, even with substantial amounts of dissolved



Figure 2. The 13 castings were produced.

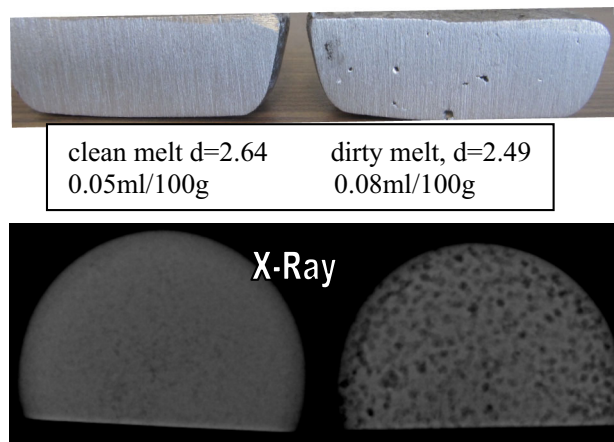


Figure 3. RPT samples of clean and dirty melts with similar low hydrogen content are pictured.

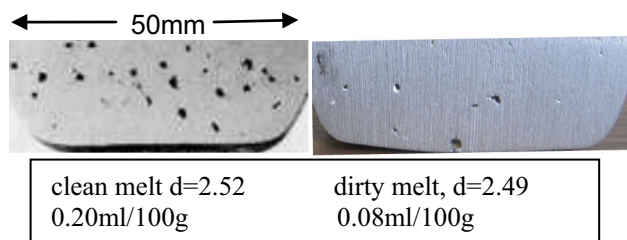


Figure 4. RPT samples of similar density are pictured.

hydrogen.⁶ On the other hand, if numerous inclusions are present, they nucleate microvoids which do not appear on the grinded section of the RPT sample. This is blatant on Figure 4 where two RPT samples of similar densities are compared. The one on the left from a gassed clean melt and the other from a degassed ‘dirty’ melt.

When the RPT sample from the ‘dirty melt’ (on the right in Figure 4) is polished to a mirror finish, the microvoids appear as shown in Figure 5. A blown-up view of part of the surface is shown on top of the same figure.

This simple comparison illustrates that the density of the RPT sample represents a combined effect of gas content and inclusions. If only the appearance of the grinded surface of the sample is considered, microvoids of ‘dirty’ melts are overlooked which may lead to erroneous conclusions.

Radiographs and Dye Penetrant

Radiographic Analyses

As illustrated in Figures 6, 7 and 8, the radiographic analysis of the LPPM cast plates showed castings of very good quality, but for the bottom part of some 25 mm (0.98 in.) plates where the early solidification in the gate resulted

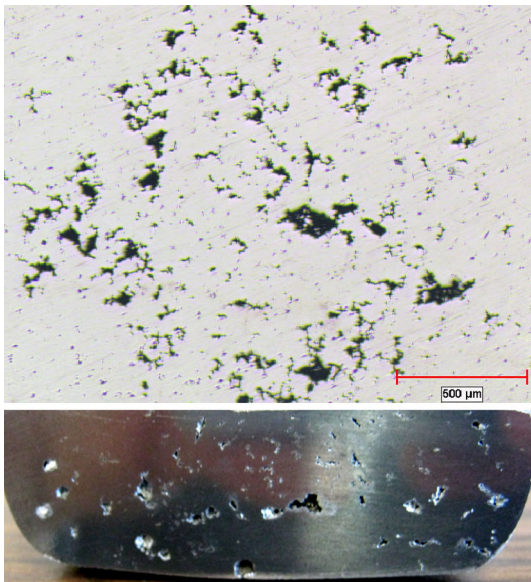


Figure 5. This is a polished 'dirty melt' RPT sample.

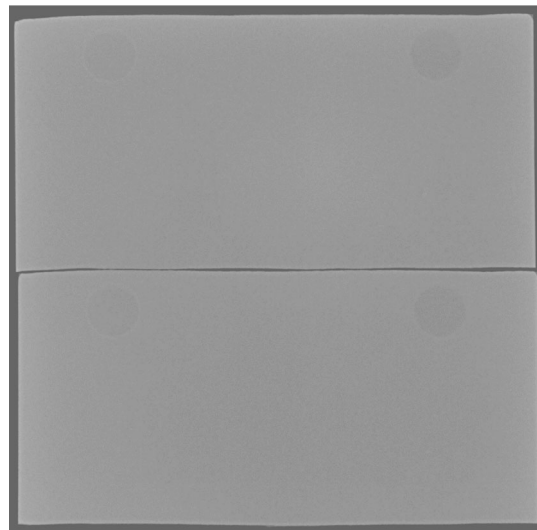


Figure 8. This is a typical radiograph, 6 mm plate (casting #6); porosity round, Frame 2 (ASTM E155).

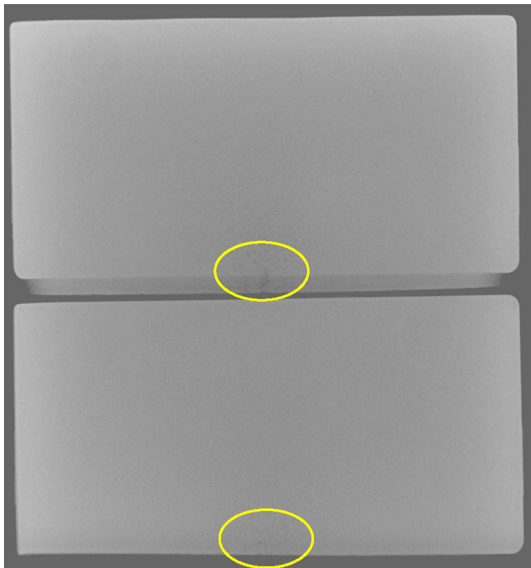


Figure 6. This is a typical radiograph of 25 mm plates (castings #1, #2); porosity round, Frame 3 (ASTM E155).



Figure 9. A dye check on the machined surface of the 25 mm plate, 80 × 160 mm (3.15 × 6.30 in.) (casting #5) is shown.

in shrinkage (i.e. Frame 3 per ASTM E155 circled in yellow in Figure 6). As expected, inclusions are not visible on the radiographs.

Since the current inclusions cannot be detected by radiography, it was decided to resort to dye penetrant.

Dye Penetrant Checks

A recognized method to detect inclusions is via dye penetrants. However, they can only detect inclusions on machined surfaces. One leftover stepped casting (#5) was used to machine out half the thickness of the 25 mm (0.98 in.) and 6 mm (0.24 in.) plates and carry out a dye penetrant inspection on these opened (machined) surfaces. Figures 9 and 10 show the defects detected by dye penetrant on the 25 mm (0.98 in.) plate. Figures 11 and 12 are equivalent to Figures 9 and 10 for the 6 mm (0.24 in.) plate of casting #2.



Figure 7. This is a typical radiograph of a 12 mm plate (casting #1); porosity round, Frame 2 (ASTM E155).

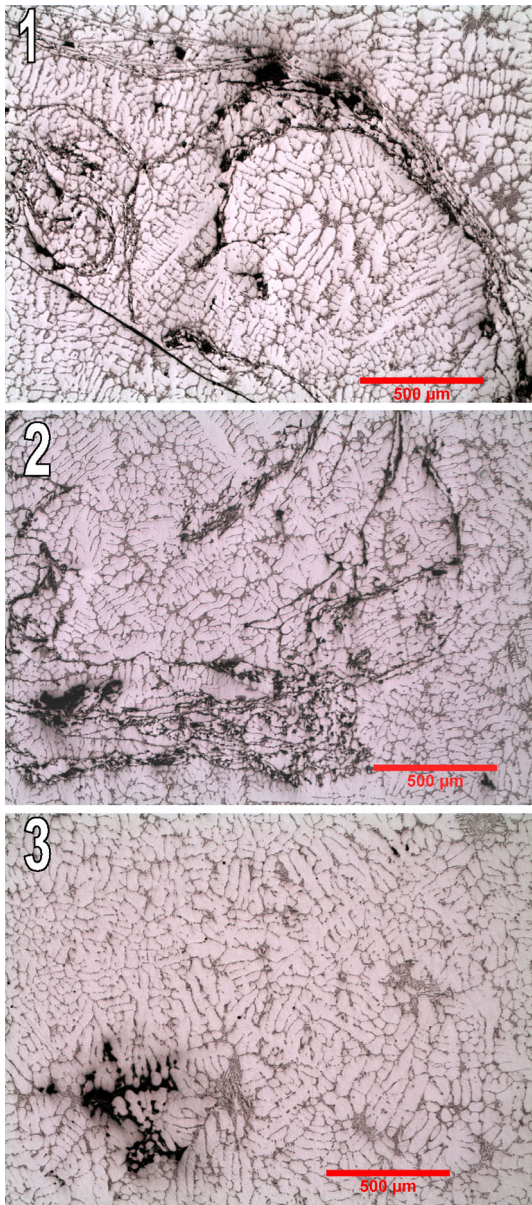


Figure 10. Micrographs of defects #1, 2, 3 in Figure 9 are pictured.

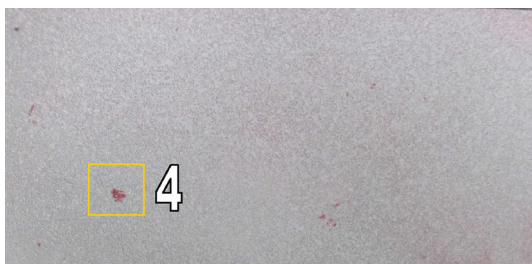


Figure 11. This is a dye check on the machined surface of a 6 mm plate, 80 × 160 mm (casting #5).

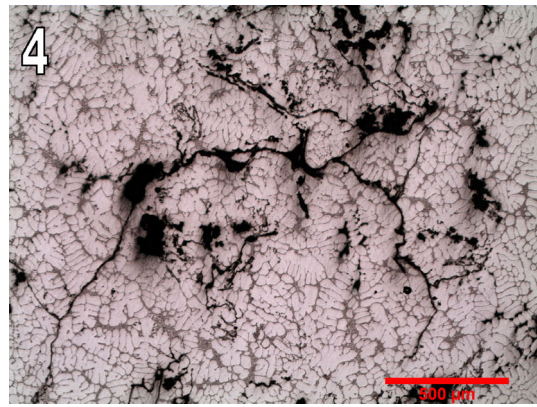


Figure 12. Micrograph of defect 4 in Figure 11 is pictured.

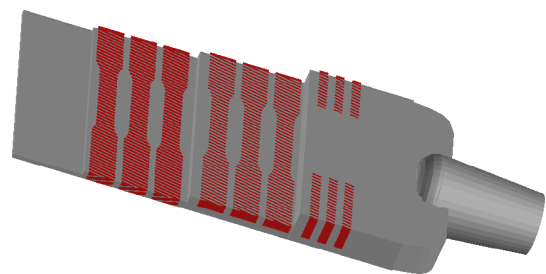


Figure 13. Location of excised tensile test bars is shown.

The appearance of the defects marked 1, 2, and 3 on Figure 9 are shown at higher magnification in Figure 10. It is confirmed that these voids have their origin in inclusions.

Measuring the Effect of Inclusions on the Tensile Properties

Figure 13 shows the sketch of a stepped casting and the locations where the flat tensile test bars [12 × 6 mm (0.47 × 0.24 in.) in section] were cut out from the 6 mm (0.24 in.), 12 mm (0.47 in.) and 25 mm (0.98 in.) thick plates.

The 54 test bars were cut from step castings poured from the same melt over a 30 min period (5 min cycle time). They were pulled after a standard T6 heat treatment [solutionized for 8 h at 540 °C (1004 °F), quenched in 65 °C (149 °F) water and then aged 6 h at 160 °C (320 °F)].

All fractured surfaces were inspected and the specimens were separated in two lots: Samples with inclusions visually detected on the fracture surface and samples without. Therefore, it was possible to evaluate the drop in tensile

properties of the exactly same alloy poured under the exact same conditions when an inclusion is the cause of the fracture.

Tensile Tests Results

The results of the tensile tests on the 54 samples are listed in Table 1. The yield strength (YS), ultimate tensile strength (UTS) and elongation (El) are shown. The quality index, $Q = UTS \text{ (MPa)} + 150 \text{ Log El\%}$ is also indicated. Q has been shown to be independent of the temper applied to the solutionized and quenched AlSiMg alloy.¹² The number of samples are indicated in bold parentheses; thus, the listed values represent the average of 8, 9 or 10 results. The standard deviation for each tensile property is shown in parentheses. These results confirm that the inclusion content does not affect the yield strength. Yield strength depends little on the thickness of the plate (i.e., on dendrite fineness and level of microporosity). On the other hand, inclusions reduce ductility with a consequent lower level of quality (Q). The relative standard deviation (SD/average) is, as expected, much less for YS than for UTS and El. It is virtually the same with and without oxides, except for YS where the standard deviation is substantially higher in the no oxides samples for the 6 mm (0.24 in.) and 25 mm (0.98 in.) plates. It must be pointed out that the YS is reached when dislocations anchoring by microprecipitates breaks up, allowing dislocation slip across the grains and hence plastic deformation. Consequently, inclusions play no role in the onset of plastic deformation, which defines the value of YS. Hence, the standard deviation should be similar in samples with and without oxides, which is clearly not the case for the 6 mm (0.24 in.) and 25 mm (0.98 in.) plates. This unexpected behavior cannot be attributed to differences in heat treatment as tensile samples with and without oxides were excised from the same heat treated step castings.

Observation of the Fracture Surfaces

Typical appearances of inclusions in the matching fractured surfaces of two tensile test bars are shown in Figures 14 and 16 (complete surfaces). The yellow rectangle in Figure 14 is enlarged in Figure 15a. Figure 15b presents

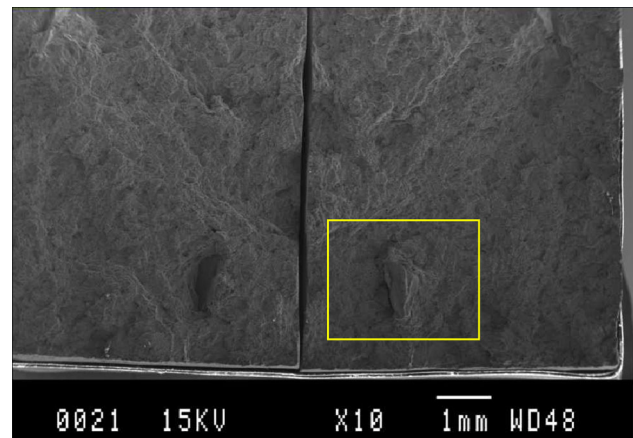


Figure 14. Matching fracture surfaces of a test bar cut in the 6 mm plate (casting #11) are shown.

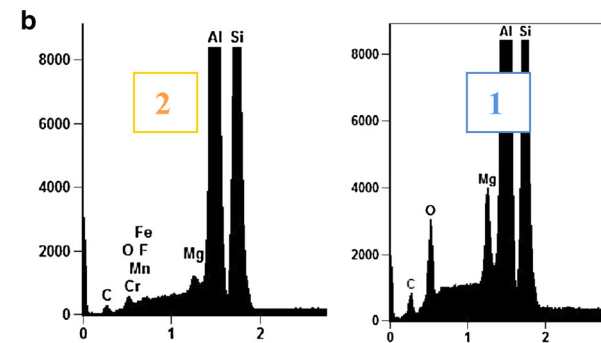
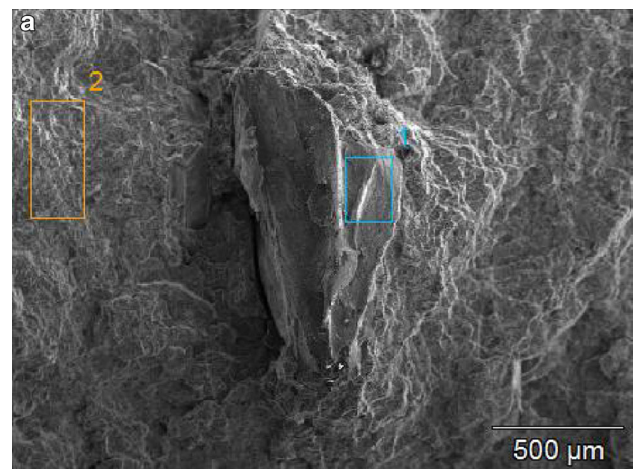


Figure 15. (a) Zoom on yellow rectangle in Figure 14 is shown. (b) Elements detected at location 1 (blue) and 2 (orange) in (a) are shown.

Table 1. Tensile Properties of Test Samples With and Without Oxide Inclusions on the Fracture Surface (SD)

	UTS (MPa)	YS (MPa)	El%	Q (MPa)
6 mm with oxides (9)	313 (12)	244 (3)	4.7 (1.8)	414
6 mm no oxides (9)	328 (15)	240 (9)	9.0 (2.9)	471
12 mm with oxides (8)	298 (24)	239 (10)	3.3 (1.1)	375
12 mm no oxides (8)	301 (21)	233 (12)	4.3 (0.9)	396
25 mm with oxides (10)	276 (16)	228 (6)	2.8 (1.2)	343
25 mm no oxides (8)	290 (15)	233 (12)	3.7 (1.4)	375

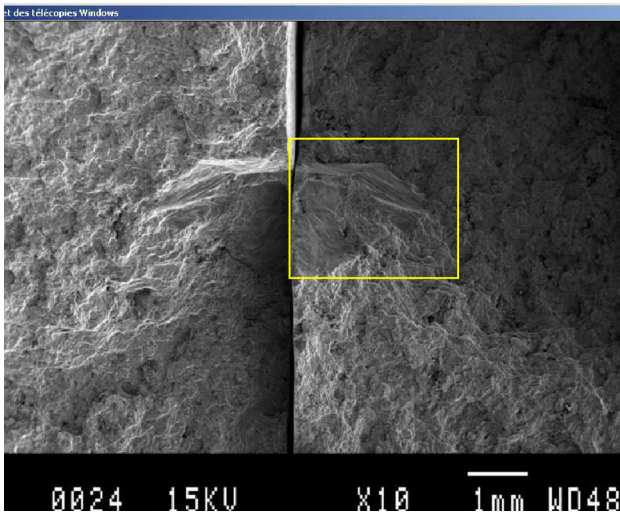


Figure 16. Matching fracture surfaces of a test bar cut in the 25 mm plate (casting #11) are shown.

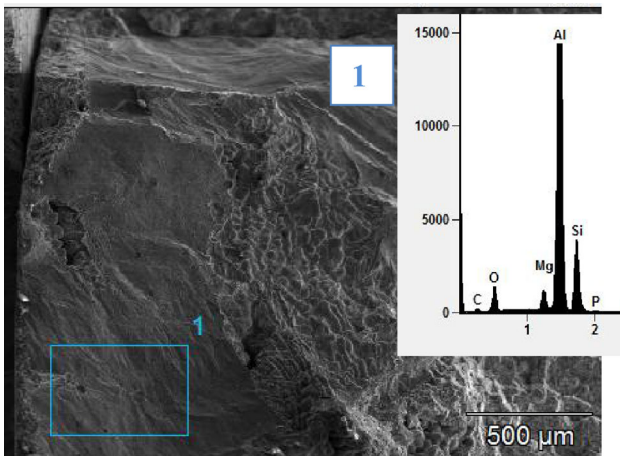


Figure 17. Zoom on yellow rectangle in Figure 16 is shown.

Energy Dispersed X-ray (EDX) diagrams showing the presence of oxide at the location identified by a blue rectangle numbered, 2.

Similarly, the two matching fractured surfaces in the 25 mm (0.98 in.) plate of the same casting are shown in Figure 16. The yellow rectangle in Figure 16 is enlarged in Figure 17; on the same figure, an EDX diagram shows the presence of oxide at the location identified by a blue rectangle numbered, 1.

Conclusions

From the present study on the effect of inclusions in aluminum A356, the following conclusions can be drawn:

1. The presence of inclusions nucleating molecular hydrogen results in an apparent high gassing in the RPT sample, even at low melt gas content.

2. Inclusions (bi-films) cannot be detected by radiographic techniques
3. Inclusions can be detected on machined surface by dye penetrant techniques.
4. Inclusions on the fracture surface may be detected by EDX on a Scanning Electron Microscopy (SEM) exposure.
5. In the 25 mm (0.98 in.) plate (solidification time ~ 54 s), the quality index was 343 MPa when an inclusion was present in the fracture surface and 375 MPa, otherwise.
6. In the 12 mm plate (solidification time ~ 31 s), the quality index was 375 MPa when an inclusion was present in the fracture surface and 396 MPa, otherwise.
7. In the 6 mm (0.24 in.) plate (solidification time ~ 10 s), the quality index was 414 MPa when an inclusion was present in the fracture surface and 471 MPa, otherwise.

The latter 3 results quantify the detrimental effect of inclusions on the static tensile properties; this effect is the most important in the fast cooling 6 mm (0.24 in.) plate.

Acknowledgments

The authors wish to acknowledge the financial support of the Natural Sciences and Engineering Research Council of Canada for funding the Chair on the Transformation of Aluminum at Centre de Métallurgie du Québec. This study would not have been possible without the close collaboration of Jeremy Carignan. Finally, the authors must recognize the valuable contribution of Olivier Jacob, an intern student from Université Laval (Québec City) for the laboratory work.

REFERENCES

1. D. Dautre, B. Gariépy, J.P. Martin, G. Dubé, Aluminum cleanliness: methods and applications in process development and quality control, in *Light Metal* (1985), pp. 1179–1195
2. L. Liu, F.H. Samuel, Assessment of melt cleanliness in A356.2 aluminum casting alloy using the porous disc filtration apparatus technique. *J. Mater. Sci.* **32**, 5927–5944 (1997)
3. A. Simard, F. Dallaire, J. Proulx, P. Rochette, Cleanliness measurement benchmarks of aluminum alloys obtained directly at-line using the PREFIL-Footerprint Instrument, in *Light Metal 2000* (The Mineral, Metals and Materials Society, 2000), pp. 739–744
4. D.P.K. Singh, D.J. Mitchell, Analysis of metal quality in a low pressure permanent mold foundry. *AFS Trans.* **109**, 333–345 (2001)
5. Alscan Brochure. [http://www05.abb.com/global/scot/scot205.nsf/veritydisplay/fc2cb792637155fd85257bf1006a9212/\\$file/Alscan_Brochure%20Hr.pdf](http://www05.abb.com/global/scot/scot205.nsf/veritydisplay/fc2cb792637155fd85257bf1006a9212/$file/Alscan_Brochure%20Hr.pdf)

6. G. Laslaz, P. Lamy, Gas porosity and metal cleanliness in aluminum casting alloys. *AFS Trans.* **99**, 83–90 (1991)
7. J. Campbell, The Bifilm concept: prospect of defect-free castings, in *Proceedings of the 68th World Foundry Congress* (2007), pp. 1–6
8. M. Stucky, Elimination of oxides in aluminium alloys: dream or reality? *Fond. Mag.* **26**, 15–26 (2012)
9. B. Eisaabadi et al., Effect of oxide films, inclusions and Fe on reproducibility of tensile properties in cast Al–Si–Mg alloys: statistical and image analysis. *Mater. Sci. Eng. A* **558**, 134–143 (2012)
10. T. Ludvig, M. Di Sabatino, L. Arnberg, Influence of oxide additions on the porosity development and mechanical properties of A356 aluminium alloy castings. *IJMC* **6**(2), 41–50 (2012)
11. J. Cheng, N. Hort, K.U. Kainer, S. Kwak, *Effects of Defects on Tensile Properties of A356 Casting Alloys*. <http://www.metal2014.com/files/proceedings/12/reports/1805.pdf>. (2013)
12. M. Drouzy, S. Jacob, M. Richard, Interpretation of tensile results by means of quality index and probable yield strength. *Int. J. Cast Metal. Res.* **5**(2), 43–50 (1980)